Received: 12 July 2020 | Revised: 12 November 2020 | Accepted: 24 November 2020

DOI: 10.1111/cas.14751

ORIGINAL ARTICLE

Cancer Science WILEY

MiR-320b/RAD21 axis affects hepatocellular carcinoma radiosensitivity to ionizing radiation treatment through DNA damage repair signaling

Jianyang Wang[1] | Hong Zhao[2] | Jing Yu[3] | Xin Xu[1] | Hao Jing[1] | Ning Li[1] | Yuan Tang[1] | Shulian Wang[1] | Yexiong Li[1] | Jianqiang Cai[2] | Jing Jin[1]

[1]Department of Radiation Oncology, National Cancer Center/National Clinical Research Center for Cancer/Cancer Hospital, Chinese Academy of Medical Sciences and Peking Union Medical College, Beijing, China

[2]Department of Hepatobiliary Surgery, National Cancer Center/National Clinical Research Center for Cancer/Cancer Hospital, Chinese Academy of Medical Sciences and Peking Union Medical College, Beijing, China

[3]Hubei Key Laboratory of Tumor Biological Behaviors, Zhongnan Hospital of Wuhan University, Wuhan, China

Correspondence

Jing Jin and Jianqiang Cai, National Cancer Center/National Clinical Research Center for Cancer/Cancer Hospital, Chinese Academic of Medical Sciences, Peking Union Medical College, No. 17 Panjiayuan Nanli, Chaoyang District, Beijing 100021, China.
Emails: jinjing@csco.org.cn and caijianqiang188@sina.com

Funding information

Chinese Academy of Medical Sciences Innovation Fund, Grant/Award Number: 2017-I2M-1-005 and 2017-I2M-2-005; National Key Research &Development Program of China, Grant/Award Number: 2016YFC0904600 and 2017YFC1311000; National Natural Science Foundation of China, Grant/Award Number: 81602168 and 81773241

Abstract

Hepatocellular carcinoma (HCC) is one of the most common malignancies in the world and is associated with high mortality. Ionizing radiation (IR)-based therapy causes DNA damage, exerting a curative effect; however, DNA damage repair signaling pathways lead to HCC resistance to IR-based therapy. RAD21 is a component of the cohesion complex, crucial for chromosome segregation and DNA damage repair, while it is still unclear whether RAD21 is implicated in DNA damage and influences IR sensitivity in HCC. The current research explores the effect and upstream regulatory mechanism of RAD21 on IR sensitivity in HCC. In the present study, RAD21 mRNA and protein expression were increased within HCC tissue samples, particularly within IR-insensitive HCC tissues. The overexpression of RAD21 partially attenuated the roles of IR in HCC by promoting the viability and suppressing the apoptosis of HCC cells. RAD21 overexpression reduced the culture medium 8-hydroxy-2-deoxyguanosine concentration and decreased the protein levels of γH2AX and ATM, suggesting that RAD21 overexpression attenuated IR treatment-induced DNA damage to HCC cells. miR-320b targeted RAD21 3′-UTR to inhibit RAD21 expression. In HCC tissues, particularly in IR-insensitive HCC tissues, miR-320b expression was significantly downregulated. miR-320b inhibition also attenuated IR treatment-induced DNA damage to HCC cells; more importantly, RAD21 silencing significantly attenuated the effects of miR-320b inhibition on IR treatment-induced DNA damage, suggesting that miR-320b plays a role through targeting RAD21. In conclusion, an miR-320b/RAD21 axis modulating HCC sensitivity to IR treatment through acting on IR-induced DNA damage was demonstrated. The miR-320b/RAD21 axis could be a novel therapeutic target for further study of HCC sensitivity to IR treatment.

KEYWORDS

DNA damage, hepatocellular carcinoma, ionizing radiation-based therapy, miR-320b, RAD21

Jianyang Wang, Hong Zhao and Jing Yu were contributed equally to this work.

1 | INTRODUCTION

Hepatocellular carcinoma (HCC) is one of the most common malignancies in the world and is associated with high mortality.[1] Despite the development of HCC treatments over the past two decades, the overall survival of HCC patients remains unsatisfactory, especially for those in advanced stages, due to recurrence and metastasis.[2,3] Radiation therapy has emerged as an alternative treatment for locally advanced HCC and the new radiation therapy strategies, such as stereotactic body radiotherapy, seem promising.[4,5] Ionizing radiation (IR) plays roles both directly and indirectly: directly damaging DNA or indirectly producing free radicals through ionization of water. Hence, various forms of DNA damage may occur, including single-strand breaks repaired through the base excision repair pathway and double-strand breaks (DSB) repaired through the homologous recombination pathway.[6] However, the resistance of tumors to IR is still a significant barrier to effective HCC treatment.[7,8] Thus, it is of great necessity to develop new strategies that can effectively improve the efficacy of radiotherapy for HCC treatment.

Cohesins are highly conserved multiprotein complexes from yeast to humans. Their main function is to bind sister chromatids closely together. This mechanism, known as sister chromatid polymerization, is the basis of various critical cellular processes, such as error-free homologous recombination repair of DNA DSB.[9-11] RAD21 is a central component of the cohesin complex, both structurally and functionally.[12] As a DNA repair gene, rad21 was first identified as radiation-sensitive mutations in the fission yeast *Schizosaccharomyces pombe*.[13,14] Recent studies suggest the potential role of RAD21 in regulating cellular growth and protecting cells from DNA damage, both of which are considered key factors in tumorigenesis. Specifically, Rad21 is involved in homologous recombination-mediated DSB repair.[15,16] In mammalian cells, RAD21 deficiency would result in sister chromatid abnormal separation in the interphase and incorrect alignment in the metaphase. In the meantime, enhanced spontaneous chromosome disruption and IR-induced chromosome aberrations also occur in these cells, possibly because of impaired DSB repair efficiency.[17] Notably, abnormal expression of RAD21 was found in a variety of cancers and cancer cells.[18-21] These observations suggest that RAD21 might facilitate IR-induced DNA damage repair, thus leading to the radioresistance of cancer. Searching for agents targeting RAD21 is a potential strategy to improve HCC radio sensitivity to IR-based therapy.

MicroRNA (miRNA) are endogenous 21-25-nucleotide (nt) noncoding small RNA that were initially regarded as "transcriptional noise."[22,23] However, published studies have shown that miRNA are involved not only in the modulation of developmentally timed events but also in the regulation of various other aspects in animal and plant biological processes.[24,25] The mature miRNA is loaded into the RNA-induced silencing complex (RISC) and binds with partial complementarity to the 3′-UTR (untranslated region) of target mRNA for degradation or translational inhibition.[26,27] Reportedly, miRNA could suppress the expression of cancer-associated genes and enable them to exert tumor-suppressive or oncogenic effects.[28-30] Notably, miRNA contribute to RAD protein regulation. The majority of the RAD proteins have the predicted miRNA binding sites in their 3′-UTR, but only RAD51 and RAD52 have been reported to exhibit miRNA regulatory effects.[31-34] Overexpression of miR-302, one of the miRNA that target RAD52, is enough to make cells sensitive to IR, possibly through inhibiting RAD52 and homologous recombination and enhancing cell apoptosis.[34] Thus, we speculate that identifying miRNA that target RAD21 might provide novel agents to improve HCC IR resistance.

Herein, we first examined the RAD21 expression level within HCC and adjacent non–cancerous tissue samples, or IR-sensitive (sensitive to IR) and IR-insensitive (insensitive to IR) HCC tissue samples, or in HCC cell lines in response to IR treatment. RAD21 overexpression was conducted within HCC cells and the impact of RAD21 on HCC cell viability, apoptosis, DNA damage, and related markers was examined with or without IR treatment. We used five online tools, including mirDIP, microT-CDS, starBase V3, TargetScan, and miRDB, to predict miRNA that could bind to RAD21, and selected miR-320b after reviewing the published literature and examining the expression levels of candidate miRNA upon IR treatment. The predicted miR-320b binding to RAD21 was validated. The impact of miR-320b on HCC cell viability, apoptosis, DNA damage, and related markers was examined with or without IR treatment. Finally, the effects of miR-320b and RAD21 on HCC sensitivity to IR treatment were examined.

2 | MATERIALS AND METHODS

2.1 | Tissue sample collection

A total of 20 paired HCC tissues and adjacent non–cancerous tissues and 24 post–radiotherapy HCC tissues were collected from patients diagnosed with HCC who had undergone surgical resection at the Cancer Hospital, Chinese Academy of Medical Sciences. All the specimens were stored at −80°C until further use in experiments. The study was conducted with the approval of the institutional review board (No. NCC2016G-047).

The IR-sensitive or IR-insensitive samples were acquired from HCC patients without distant metastasis who had undergone radical radiotherapy. The total dose of administered radiotherapy for HCC patients ranged from 12 to 60 Gy (1.8–5.0 Gy/fraction, 5 days/week, followed by rest for 2 days). The total dose was determined by radiation oncologists, based on age, performance status, liver function, and dose volume of the normal liver, duodenum, and stomach.[35] The clinical evaluation of radiosensitivity in HCC patients is based on the first re–examination of CT scans after undergoing radiotherapy for 1 month, according to the following criteria: patients with radioresistant HCC patients were defined as those with persistent disease at >3 months, or with local recurrent disease in the liver or both within 12 months of completion of radiotherapy.[36,37] According to the evaluation, 12 samples were IR-sensitive and 12 were IR-insensitive.

2.2 | H&E staining

Tissue samples were fixed with 4% paraformaldehyde, embedded, and then sliced into 5-μm thick sections. Then, slices were dewaxed, hydrated, and stained with H&E. Histopathological changes were observed under a light microscope.

2.3 | Immunohistochemistry staining

Tissue sections described above were dewaxed, hydrated, and incubated with 0.01 mol/L sodium citrate buffer solution (pH = 6.0) by steaming for 30 minutes, and then immersed in 100 μL hydrogen peroxide (3%) for 15 minutes at room temperature. Sections were then incubated with primary antibodies, anti–RAD21 (csb-PA040139; CUSABIO), or anti–Ki-67 (27309-1-AP; Proteintech) at 4°C overnight. Depending on the primary antibody, anti–mouse or anti–rabbit IgG coupled with peroxidase was used as a secondary antibody. Section visualization was conducted through incubation with DAB solution and weak counterstaining with hematoxylin. Under a light microscope, five fields (×400) were randomly selected and the positive cells were counted.

2.4 | PCR analysis

Total RNA was extracted from target cells using TRIzol Reagent (Invitrogen). The relative expression levels of target factors were determined using the SYBR Green PCR Master Mix (Qiagen) according to the protocols. GAPDH expression (for mRNA expression determination) or RNU6B expression (for miRNA expression determination) was used as an endogenous normalization control. The relative expression levels were calculated using the $2^{-\Delta\Delta CT}$ method. The primer sequences for the PCR assay are listed in Table 1.

2.5 | Immunoblotting

The protein levels of RAD21, γH2AX, ATM, and Ki-67 were detected using immunoblotting. Target cells were lysed in RIPA buffer with 1% PMSF for protein extraction. Proteins were loaded onto an SDS-PAGE minigel and transferred onto PVDF membranes followed by incubation with anti–RAD21 (csb-PA040139; CUSABIO), anti–γH2AX (10856-1-AP, Proteintech), anti–ATM (ab78, Abcam), or anti–Ki-67 (27309-1-AP, Proteintech) at 4°C overnight, and subsequently incubated with the HRP-conjugated secondary antibody. ECL Substrates was used to visualize signals (Millipore). β-actin was used as an endogenous protein for normalization.

2.6 | Cell lines and cell transfection

The HCC cell line Hep3B was obtained from the ATCC (HB-8064) and cultured in Eagle's minimum essential medium (Catalog No. 30-2003; ATCC) supplemented with 10% FBS (Invitrogen). HCC cell line Huh7 was purchased from the China Center for Type Culture Collection (3111C0001CCC000679; CCTCC) and cultured in DMEM-H: DMEM (DME H-21 4.5g/Liter Glucose) supplemented with 10% FBS (Invitrogen).

TABLE 1 The primer sequence for PCR assay

Gene	Primer	Sequence
RAD21	Forward	5′-GGATAAGAAGCTAACCAAAGCCC-3′
	Reverse	5′-CTCCCAGTAAGAGATGTCCTGAT-3′
miR-212-3p	Forward	5′-GCCGTAACAGTCTCCAGTC-3′
	Reverse	5′-CAGTGCGTGTCGTGGA-3′
miR-363-3p	Forward	5′-GGAATTGCACGGTATCCA-3′
	reverse	5′-CAGTGCGTGTCGTGGA-3′
miR-299-5p	Forward	5′-GCTGGTTTACCGTCCCAC-3′
	Reverse	5′-CAGTGCGTGTCGTGGA-3′
miR-320b	Forward	5′-GCAAAAGCTGGGTTGAGA-3′
	Reverse	5′-CAGTGCGTGTCGTGGA-3′
miR-367-3p	Forward	5′-GCCAATTGCACTTTAGCAA-3′
	Reverse	5′-CAGTGCGTGTCGTGGA-3′
miR-433-3p	Forward	5′-GGATCATGATGGGCTCCT-3′
	Reverse	5′-CAGTGCGTGTCGTGGA-3′
GAPDH	Forward	5′-ACAGCCTCAAGATCATCAGC-3′
	Reverse	5′-GGTCATGAGTCCTTCCACGAT-3′
U6	Forward	5′-CTCGCTTCGGCAGCACA-3′
	Reverse	5′-TCATCCAAATACTCCACACGC-3′

RAD21 overexpression in target cells was conducted by transfecting RAD21-overexpressing plasmid (GenePharma, Shanghai, China). miR-320b overexpression or inhibition was achieved by transfecting agomir-320b or antagomir-320b (GenePharma) using Lipo3000 (Invitrogen) for 24 hours before radiation treatment according to the manufacturer's instructions.

For IR treatment on HCC cells, Hep3B and Huh7 cells (transfected or non–transfected), were exposed to 0, 2, 4, 6, 8, or 10 Gy IR using a 6-MV X-ray generated by a linear accelerator following the methods that we used previously.[36,37] Then, the cells were cultured for 48 hours for the subsequent experiments.

2.7 | Cell viability determined by MTT assay

Target cells were seeded into 96-well plates (5×10^3 cells/well) and incubated for 24 hours. Then, cells were transfected (or not); 48 hours after transfection, 20 μL MTT (Sigma-Aldrich) was added, and the cells were incubated for an additional 4 hours in a humidified incubator. After discarding the supernatant, 200 μL DMSO was added for dissolving the formazan. The $OD_{490\ nm}$ value was measured. Cell viability in each group was calculated, normalizing to the control group.

2.8 | Cell apoptosis determined by flow cytometry

Cells were stained using PI and Annexin V-FITC for the detection of the cell apoptosis by flow cytometry following the methods we used previously.[36,37] Data were analyzed using BD FACS Diva software V6.1.3 (BD Biosciences).

2.9 | DNA damage evaluation by detecting 8-hydroxy-2-deoxyguanosine level

The levels of 8-hydroxy-2-deoxyguanosine (8-OHdG) in the culture medium were measured by 8-OHdG ELISA kit (ab201734, Abcam) following the instructions of the manufacturer. Absorbance values were measured on a microplate reader.

2.10 | Luciferase activity

To verify the predicted miR-320b binding to RAD21 3′-UTR, the present study constructed wild-type and mutated RAD21 3′-UTR luciferase reporter plasmids (wt-RAD21 3′-UTR/mut-RAD21 3′-UTR); mut-RAD21 3′-UTR contained a 5-bp mutation in the predicted miR-320b binding site. HEK293 cells (ATCC) were co–transfected with wt-RAD21 3′-UTR/mut-RAD21 3′-UTR plasmids and agomir-320b/antagomir-320b. Luciferase assays were performed to determine the luciferase activity 48 hours after transfection using the Dual-Luciferase Reporter Assay System (Promega).

2.11 | Animal study

Athymic nude mice (4-6 weeks old, from the SLAC Experimental Animal Center, Changsha, China) were used for tumor implantation following the methods described previously[38] and in accordance with the Regulations for the Administration of Affairs Concerning Experimental Animals and the Chinese National Guidelines for animal experiment, issued in 1988. All the procedures involving animals and their care were approved and performed by the Chinese Academy of Medical Sciences Animal Care and Use Committee (No. NCC2016A019). First, siRNA of RAD21 (si-RAD21) was performed using shRNA lentiviral particles (GeneChem), which were designed to knock down the production of RAD21 in Hep3B cells. Then, for xenograft tumor assays, 5×10^6 Hep3B cells co–transfected with antagomir-320b + si-RAD21 were subcutaneously injected into the back of nude mice. Transfection mice were divided into two groups. One group had no additional treatment and the other group received the following treatment: 10 days after the injection, the subcutaneous tumor was irradiated with IR at 6 Gy/time/day, once every other day, a total of 10 times. After the last irradiation, the mice were fed for another 5 days. All the mice were killed 35 days after injection; the tumors were removed for photographing and the tumor volumes were calculated.

2.12 | Statistical analyses

Data of results from at least three independent experiments are processed using GraphPad and presented as the mean ± SD. A Student *t* test was used for statistical comparison between means where applicable. Differences among more than two groups in the above assays were estimated using one-way ANOVA followed by Tukey's test. $P < .05$ was considered statistically significant.

3 | RESULTS

3.1 | RAD21 expression is upregulated within hepatocellular carcinoma tissues and ionizing radiation-insensitive hepatocellular carcinoma tissue samples

First, the study collected clinical tissue samples and examined the expression of RAD21 in tissue samples. The histopathological characteristics of tissue samples were evaluated by H&E staining; as shown in Figure 1A, H&E staining of tumor tissues revealed obvious necrosis. In tumor tissue samples, RAD21 protein (Figure 1B) and mRNA (Figure 1C) expression were dramatically increased within HCC tissue samples compared to those in adjacent normal control tissue samples. Next, after IR-based radiotherapy, the sensitivity of patients to IR was evaluated as described in methods section. The results of immunohistochemistry (IHC) staining and western blot assay showed that the protein contents of RAD21 were higher in

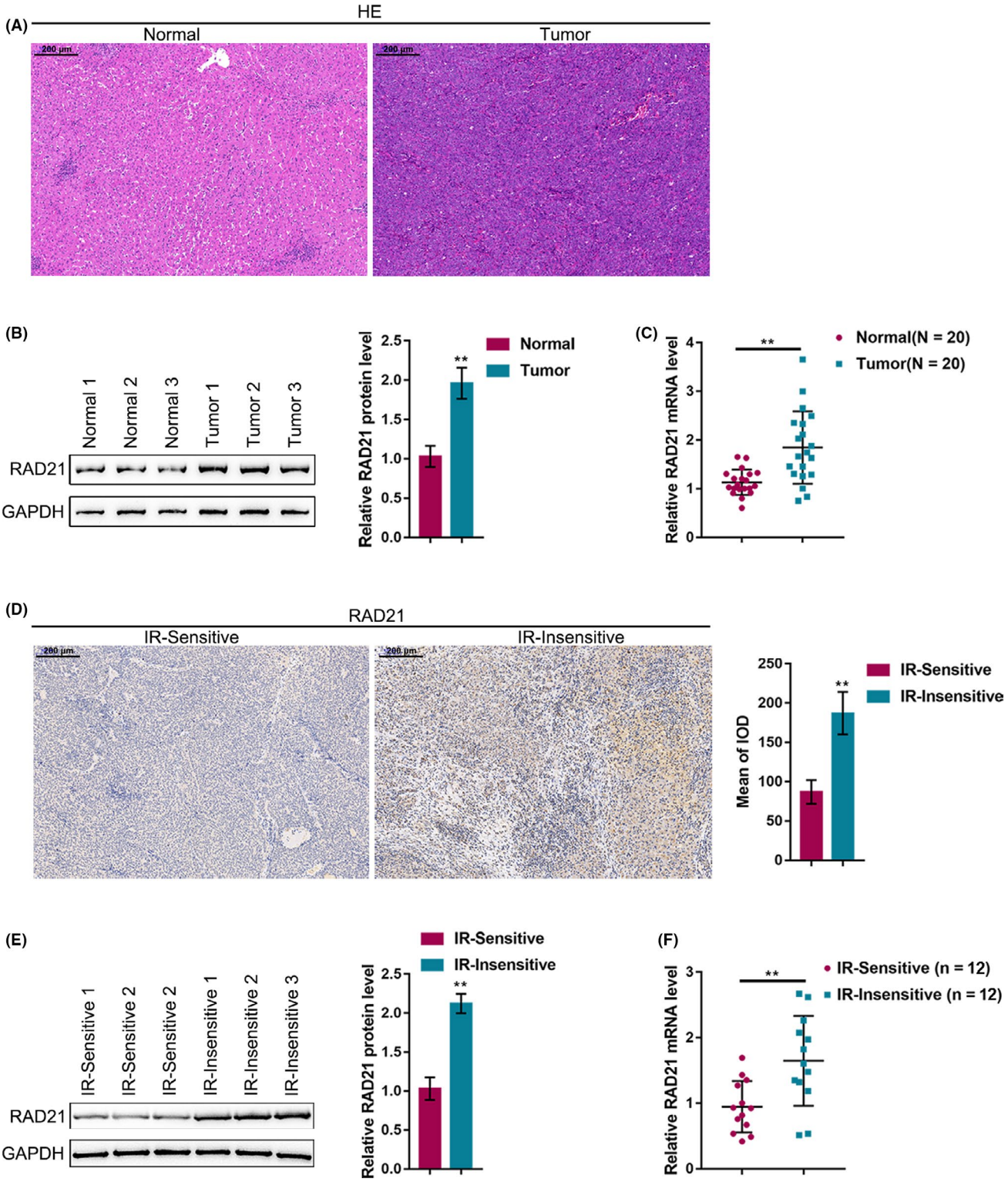

FIGURE 1 RAD21 expression is upregulated in ionizing radiation (IR)-insensitive hepatocellular carcinoma (HCC) tissue samples A, The histopathological characteristics of normal non–cancerous tissues and HCC tissues was evaluated by H&E staining. B, Three pairs of HCC and adjacent non–cancerous tissues were randomly chosen from 20 pairs of HCC and adjacent non–cancerous tissues and RAD21 protein levels in HCC and adjacent non–cancerous tissues were determined by immunoblotting. C, RAD21 mRNA expression in HCC and adjacent non–cancerous tissues was determined by real-time quantitative PCR (qPCR) (n = 20). $^{**}P < .01$ compared to normal group. D and E, Three pairs of samples of ionizing radiation (IR)-insensitive and IR-sensitive HCC tissues were randomly selected from 12 pairs of samples of IR-insensitive and IR-sensitive HCC tissues. Then, RAD21 protein content and distribution in IR-sensitive and IR-insensitive HCC tissue samples were determined by immunohistochemistry (IHC) staining or western blot assay. F, RAD21 mRNA expression in IR-sensitive and IR-insensitive HCC tissue samples was detected by real-time qPCR (n = 12). Student's *t* test was applied for statistical analysis; $^{**}P < .01$ compared to IR-sensitive group

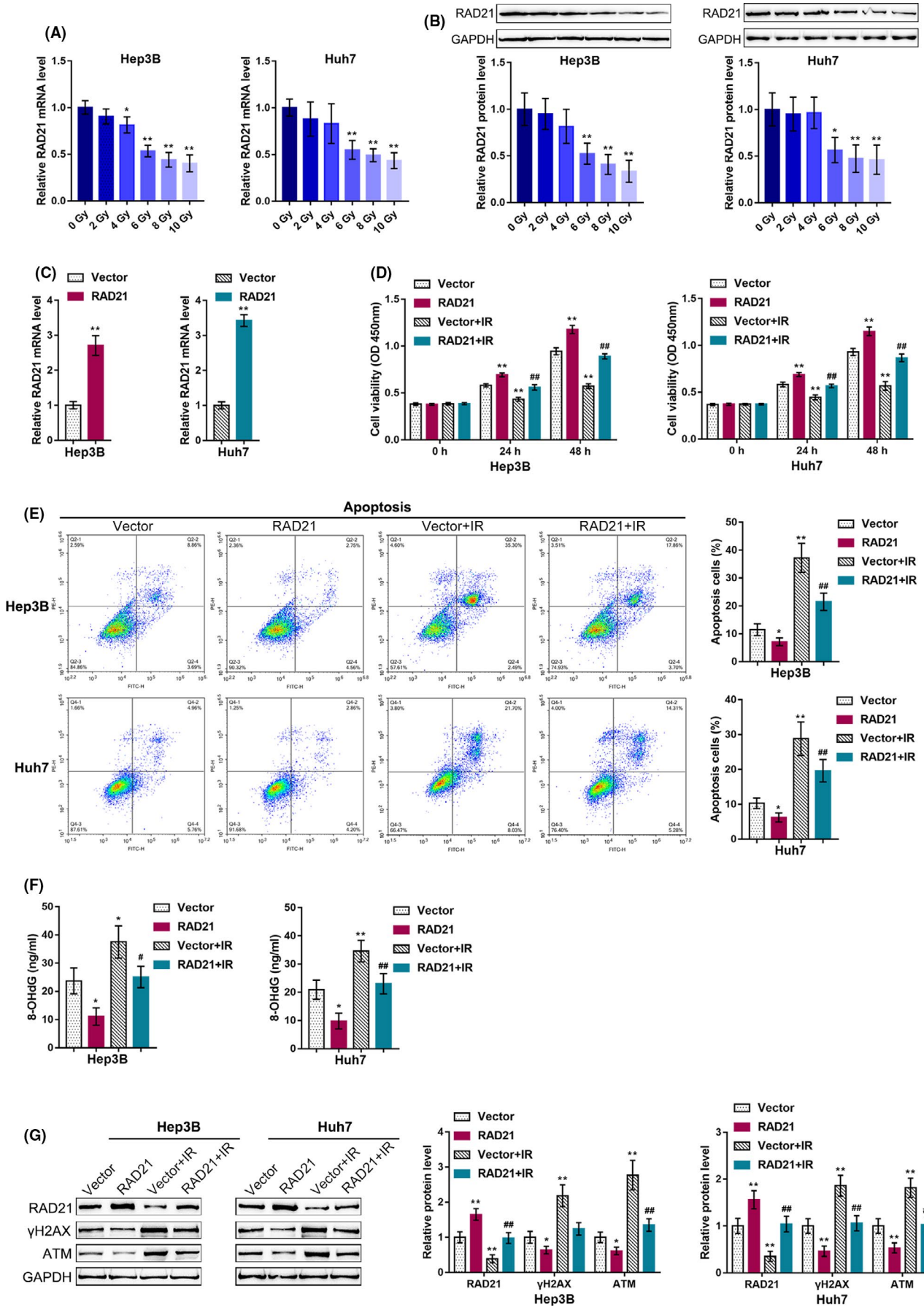
(A)
Hep3B
Huh7
Relative RAD21 mRNA level
0 Gy
2 Gy
4 Gy
6 Gy
8 Gy
10 Gy
(B)
RAD21
GAPDH
Relative RAD21 protein level
(C)
Vector
RAD21
(D)
Vector
RAD21
Vector+IR
RAD21+IR
Cell viability (OD 450nm)
0 h
24 h
48 h
(E)
Apoptosis
Vector
RAD21
Vector+IR
RAD21+IR
Apoptosis cells (%)
(F)
8-OHdG (ng/ml)
(G)
RAD21
γH2AX
ATM
GAPDH
Relative protein level

FIGURE 2 Effects of RAD21 on hepatocellular carcinoma (HCC) cell sensitivity to ionizing radiation (IR). Hep3B and Huh7 cells were exposed to different doses of IR (0, 2, 4, 6, 8, or 10 Gy) and examined. A, mRNA expression of RAD21 by real-time quantitative PCR. B, Protein levels of RAD21 by immunoblotting. At over 6 Gy IR treatment, RAD21 expression was significantly downregulated; thus, 6 Gy IR treatment was used in further experiments. C, RAD21 overexpression was conducted in Hep3B and Huh7 cells by transfecting RAD21-overexpressing plasmid (RAD21 in the figure). The transfection efficiency was verified by real-time quantitative PCR. Next, hepatocellular carcinoma (HCC) cells were transfected with RAD21 with or without 6 Gy IR treatment and examined for (D) cell viability by MTT assay. E, Cell apoptosis by flow cytometry assay. F, The concentration of 8-OHdG in the culture medium by ELISA. G, The protein levels of RAD21, γH2AX, and ATM by immunoblotting. Student's *t* test and one-way ANOVA followed by Tukey's test were applied for statistical analysis; $^{*}P < .05$, $^{**}P < .01$, compared to vector (control) group; $\#P < .05$, $\#\#P < .01$, compared to vector + IR group

IR-insensitive HCC tissues compared to those in IR-sensitive HCC tissues (Figure 1D,E). RAD21 mRNA expression was noticeably upregulated in IR-insensitive HCC tissues (n = 12) when compared to IR-sensitive HCC tissues (Figure 1F). In summary, the increase in RAD21 could be associated with HCC IR insensitivity.

3.2 | Effects of RAD21 on hepatocellular carcinoma cell sensitivity to ionizing radiation

To examine the speculation that RAD21 upregulation might be related to HCC IR insensitivity, the study exposed two HCC cell lines, Hep3B and Huh7, to different IR doses (0, 2, 4, 6, 8, or 10 Gy) and examined related indexes. As revealed by real-time quantitative PCR (qPCR) and immunoblotting, RAD21 mRNA and protein expression were downregulated via IR treatment in dose-dependent manner (Figure 2A,B). Under 6 Gy IR treatment, within both cell lines, RAD21 mRNA expression and protein levels were markedly downregulated (Figure 2A,B); thus, 6 Gy IR treatment was used in further experiments.

Next, RAD21 overexpression was conducted in Hep3B and Huh7 cells by transfecting RAD21-overexpressing plasmid (RAD21), as confirmed by real-time qPCR (Figure 2C). In both cell lines, IR treatment inhibited cell viability and enhanced cell apoptosis, whereas RAD21 overexpression exerted an opposite effect (Figure 2D,E); RAD21 overexpression could attenuate IR treatment-caused suppression upon the proliferation of HCC cells (Figure 2D,E). IR treatment increased, whereas RAD21 decreased 8-OHdG concentration in the culture medium; RAD21 overexpression reduced the IR treatment-caused increase in 8-OHdG concentration in the culture medium (Figure 2F). Moreover, as for the DNA damage markers, IR treatment decreased the RAD21 protein level and elevated the γH2AX and ATM protein content (Figure 2G), whereas RAD21 overexpression increased the RAD21 protein level and decreased the protein levels of γH2AX and ATM (Figure 2G). In summary, RAD21 overexpression could attenuate IR treatment-caused DNA damage to HCC cells, therefore reducing HCC cell sensitivity to IR treatment.

3.3 | miR-320b binds RAD21 3′-UTR to inhibit RAD21 expression

miRNA could serve as a tumor suppressor by targeting the 3′-UTR of oncogenes to suppress their expression.[39] Thus, the study used five online tools, including mirDIP, microT-CDS, starBase V3, Targetscan, and miRDB, to predict miRNA that might target RAD21; a total of 17 miRNA were identified (Figure 3A). According to previous studies, six tumor-suppressive miRNA, hsa-miR-212-3p,[40] hsa-miR-363-3p,[41] hsa-miR-299-5p,[42] hsa-miR-320b,[43] hsa-miR-367-3p,[44] and hsa-miR-433-3p,[45] were chosen for further experiments. To further confirm the candidate miRNA, the study exposed Hep3B and Huh7 cells to 6 Gy IR treatment and examined the expression levels of these six miRNA; Figure 3B shows that IR treatment significantly upregulated miR-320b expression in both cell lines. Thus, miR-320b was chosen for further experiments.

The expression of miR-320b was dramatically downregulated within HCC tissue samples compared to within adjacent normal control tissue samples (Figure 3C) and was downregulated in IR-insensitive HCC tissue samples compared to within IR-sensitive HCC tissue samples (Figure 3D). To verify the predicted miR-320b binding to RAD21 3′-UTR, the study conducted miR-320b overexpression or inhibition in Hep3B and Huh7 cells by transfecting agomir-320b or antagomir-320b, as confirmed by real-time qPCR (Figure 3E). Within both Hep3B and Huh7 cells, the overexpression of miR-320b was remarkably downregulated, whereas the inhibition of miR-320b was upregulated the RAD21 protein level (Figure 3F). Second, two different types of RAD21 3′-UTR luciferase reporter plasmids, wild-type and mutant-type (wt-RAD21 3′-UTR/mut-RAD21 3′-UTR), were constructed to perform the luciferase reporter assay. The targeted relationship between miR-320b and RAD21 was confirmed by luciferase reporter assay (Figure 3G). In summary, miR-320b targets RAD21 to inhibit RAD21 expression.

3.4 | Effects of miR-320b on hepatocellular carcinoma cell sensitivity to ionizing radiation

miR-320b downregulation in IR-insensitive HCC tissues suggests the underlying effect of miR-320b on the sensitivity of HCC cells to IR. To validate the specific effect of miR-320b, the study transfected Hep3B and Huh7 cells with antagomir-320b with or without 6 Gy IR treatment and examined related indexes. miR-320b inhibition significantly promoted the viability and suppressed the apoptosis of HCC cells, whereas IR treatment exerted an opposite effect; miR-320b inhibition could significantly attenuate the impact of IR treatment (Figure 4A,B). Regarding IR-caused DNA damage, IR treatment increased whereas miR-320b inhibition decreased the culture medium 8-OHdG concentration; miR-320b inhibition could significantly attenuate the effects of IR treatment on culture medium 8-OHdG concentration (Figure 4C).

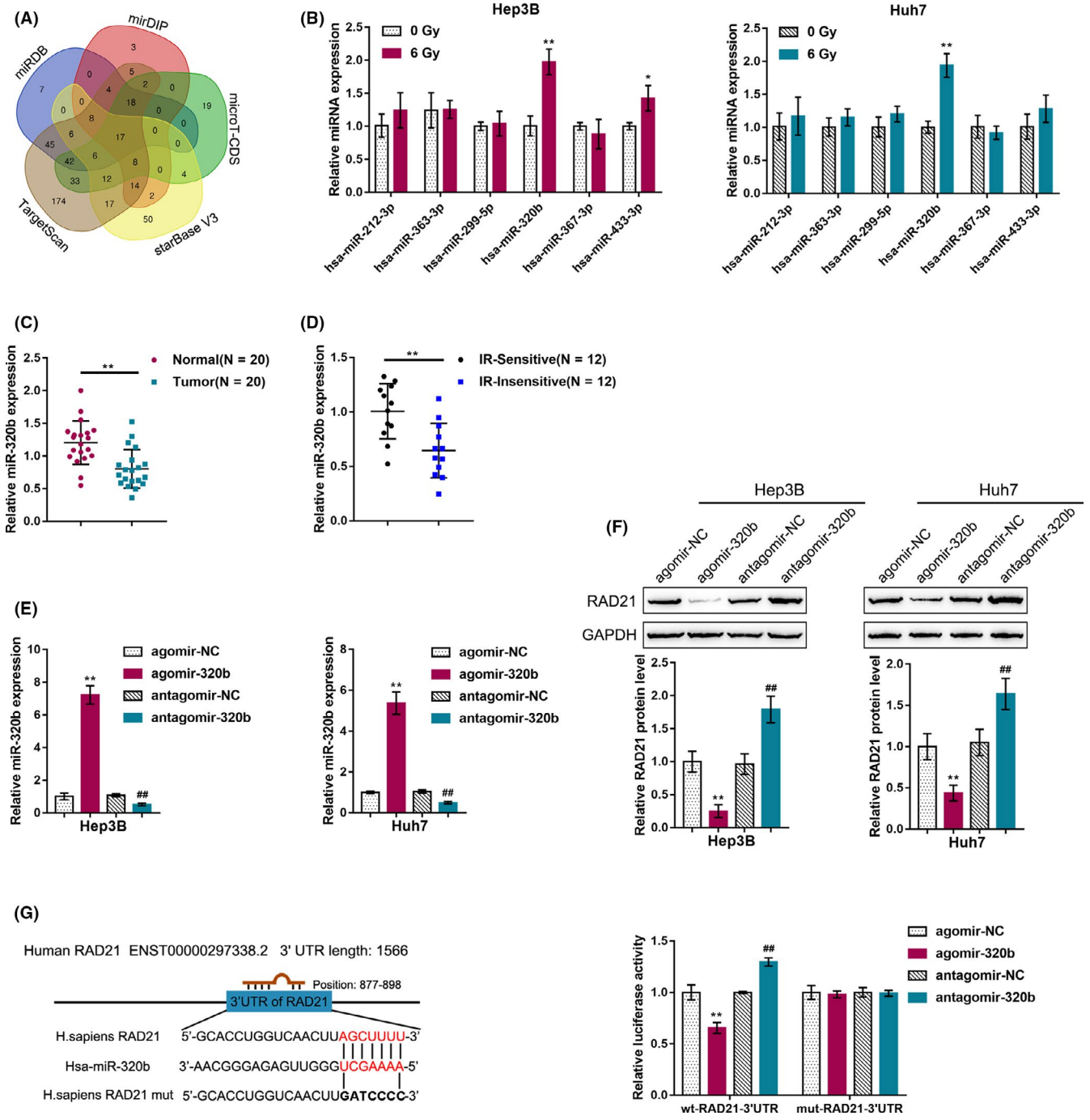

FIGURE 3 miR-320b binds RAD21 3′-UTR to inhibit RAD21 expression. A, A schematic diagram showing the process of five online tools predicting RAD21-targeted miRNA. A total of 17 miRNA were identified. B, Hep3B and Huh7 cells were exposed to 6 Gy ionizing radiation (IR) treatment and examined for the expression of hsa-miR-212-3p, hsa-miR-363-3p, hsa-miR-299-5p, hsa-miR-320b, hsa-miR-367-3p, and hsa-miR-433-3p by real-time quantitative PCR (qPCR). $^{*}P < .05$, $^{**}P < .01$ compared to 0 Gy IR treatment group. C, miR-320b expression was determined in 20 paired hepatocellular carcinoma (HCC) and adjacent non–cancerous tissue samples by real-time qPCR. Student's *t* test was applied for statistical analysis; $^{**}P < .01$ compared to normal group. D, miR-320 expression was determined in 12 IR-sensitive and 12 IR-insensitive HCC tissues by real-time qPCR. Student *t* test was applied for statistical analysis; $^{**}P < .01$ compared to IR-sensitive group. E, The transfection efficiency of agomir-320b or antagomir-320b conducted in Hep3B and Huh7 cells was verified by real-time qPCR. F, The effect of miR-320b on RAD21 protein level was detected by immunoblotting. G, Wild-type and mutant-type RAD21 3′-UTR luciferase reporter plasmids (wt-RAD21 3′-UTR/mut-RAD21 3′-UTR) were constructed and co–transfected in 293T cells with agomir-320b or antagomir-320b. The luciferase activity was determined. One-way ANOVA followed by Tukey's test was applied for statistical analysis; $^{**}P < .01$ compared to agomir-NC group; $^{\#\#}P < .01$ compared to antagomir-NC group

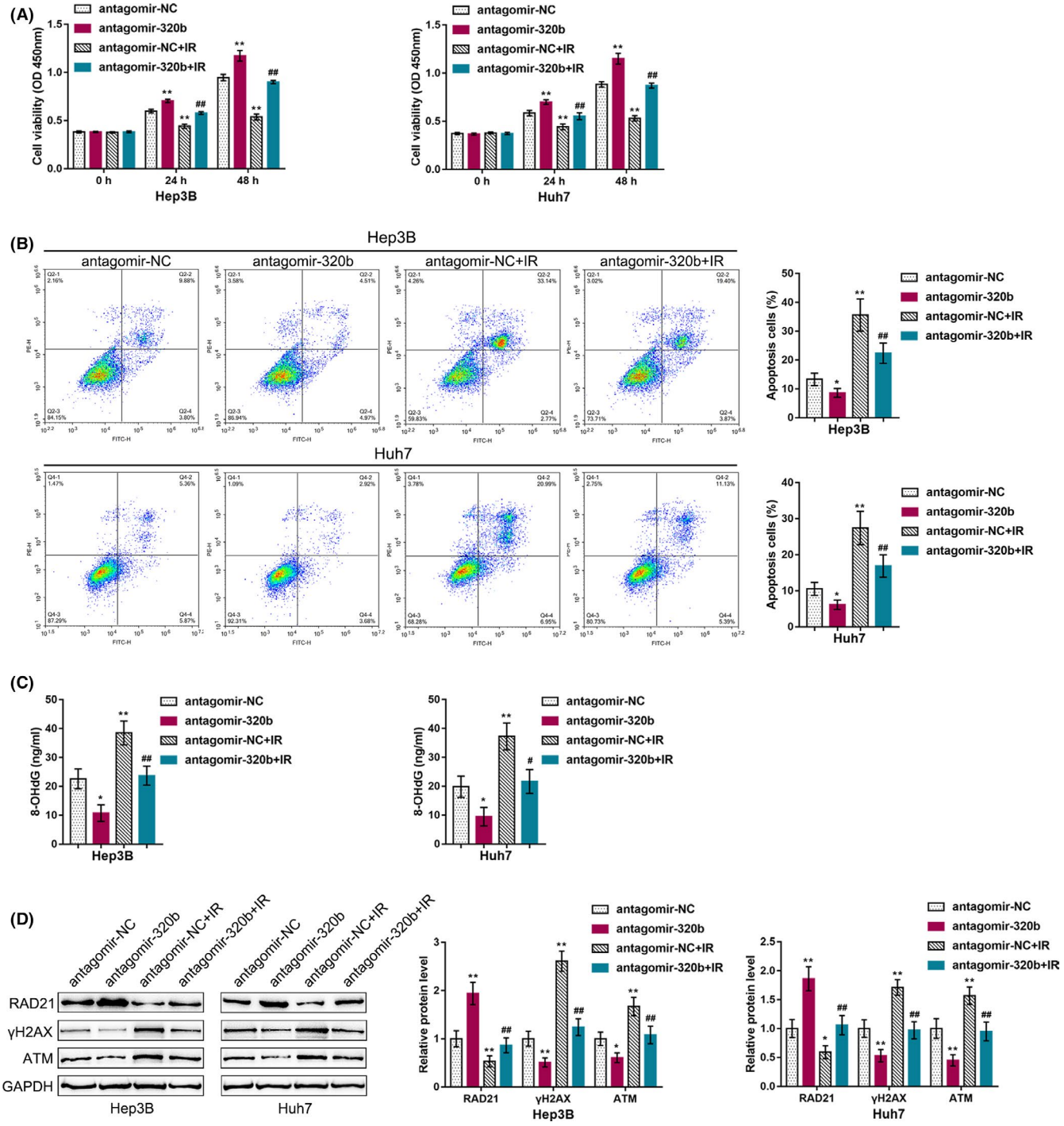

FIGURE 4 Effects of miR-320b on hepatocellular carcinoma (HCC) cell sensitivity to ionizing radiation (IR) Hep3B and Huh7 cells were transfected with antagomir-320b with or without 6 Gy IR treatment and examined for (A) cell viability by MTT assay. B, Cell apoptosis by flow cytometry assay. C, The concentration of 8-OHdG in the culture medium by ELISA. D, The protein levels of RAD21, γH2AX, and ATM by immunoblotting. One-way ANOVA followed by Tukey's test was applied for statistical analysis; $^{*}P < .05$, $^{**}P < .01$, compared to antagomir-negative control (NC) group; $\#P < .05$, $\#\#P < .01$, compared to antagomir-NC + IR group

Consistently, IR treatment decreased the RAD21 protein level and increased γH2AX and ATM protein levels, while miR-320b inhibition increased the RAD21 protein level and decreased γH2AX and ATM protein levels; miR-320b inhibition could significantly attenuate the effects of IR treatment on these proteins (Figure 4D). In summary, miR-320b inhibition could attenuate HCC IR sensitivity.

3.5 | miR-320b exerts its biological effects through RAD21

After confirming the effects of miR-320b and RAD21, respectively, on HCC cell IR sensitivity, the study continued to investigate the effects of the miR-320b/RAD21 axis. We co–transfected

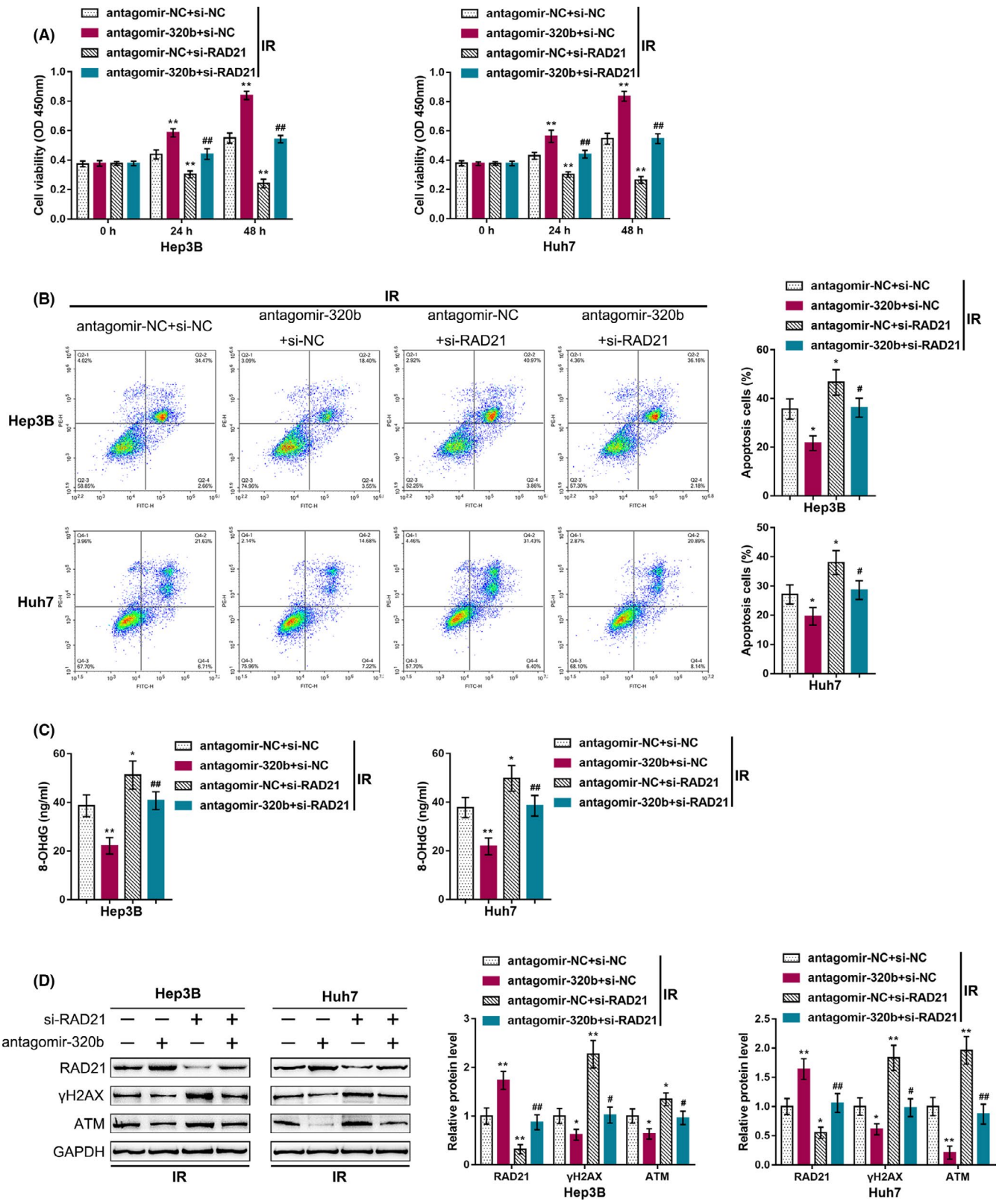

FIGURE 5 miR-320b exerts its biological effects through RAD21 under ionizing radiation (IR) treatment. Hep3B and Huh7 cells were co–transfected with antagomir-320b and lentivirus mediated si-RAD21 under 6 Gy IR treatment and examined for (A) cell viability by MTT assay. B, Cell apoptosis by flow cytometry assay. C, The concentration of 8-OHdG in the culture medium by ELISA. D, The protein levels of RAD21, γH2AX, and ATM by immunoblotting. One-way ANOVA followed by Tukey's test was applied for statistical analysis; $^{*}P < .05$, $^{**}P < .01$, compared to antagomir-negative control (NC) + si-NC group; $\#P < .05$, $\#\#P < .01$, compared to antagomir-NC + si-RAD21 group

Hep3B and Huh7 cell lines with antagomir-320b and si-RAD21 in response to 6 Gy IR treatment and determined related indexes. Under IR treatment, miR-320b inhibition significantly promoted the viability and inhibited the apoptosis of HCC cells, whereas RAD21 silencing exerted an opposite effect; RAD21 silencing partially relieved the impact of miR-320b inhibition in HCC cells (Figure 5A,B). Under IR treatment, miR-320b inhibition decreased, whereas RAD21 silencing increased the culture medium 8-OHdG concentration; the effects of miR-320b inhibition on culture medium 8-OHdG concentration were partially weakened by RAD21 silencing (Figure 5C). Under IR treatment, miR-320b inhibition increased the RAD21 protein level and decreased γH2AX and ATM protein levels, while RAD21 silencing decreased the RAD21 protein level and increased γH2AX and ATM protein levels; the roles of miR-320b inhibition in these proteins were partially attenuated by RAD21 silencing (Figure 5D). In summary, miR-320b contributes to HCC cell IR sensitivity through targeting RAD21, and RAD21 could reverse the impact of miR-320b on HCC IR sensitivity.

In addition, the combined effect of the miR-320b/RAD21 axis on normal HCC cells was also investigated. Hep3B and Huh7 cell lines were co–transfected with antagomir-320b and/or si-RAD21. Knockdown of miR-320b markedly increased cell viability and suppressed the cell apoptosis of HCC cells, while silence of RAD21 showed the opposite effect of miR-320b inhibition (Figure S1A-B). miR-320b inhibition dramatically inhibited, while RAD21 silencing increased culture medium 8-OHdG concentration in Hep3B and Huh7 cells (Figure S1C). Inhibition of miR-320b notably promoted the RAD21 protein level and restrained γH2AX and ATM protein levels, while knockdown of RAD21 suppressed the RAD21 protein level and increased γH2AX and ATM protein levels (Figure S1D).

3.6 | Effects of miR-320b/RAD21 axis on the growth of xenograft formed of hepatocellular carcinoma in vivo

As a further confirmation of the above-described findings, we established the tumor xenograft model in nude mice as described and then performed IR treatment on mice in different groups. As shown in Figure 6A, under IR treatment, the tumor volume and weight of tumors derived from miR-320b-inhibited HCC cells were significantly increased, while those of tumors derived from RAD21-silenced HCC cells were decreased; the effects of miR-320d on tumor growth were partially reversed by RAD21 silencing. As for the molecular changes, the protein levels of Ki-67 and RAD21 were dramatically increased, and γH2AX and ATM protein levels were decreased in tumors derived from miR-320b-inhibited HCC cells. In tumors derived from RAD21-silenced HCC cells, the protein levels of Ki-67 and RAD21 were dramatically decreased, and γH2AX and ATM protein levels were increased (Figure 6B). In tumors derived from antagomir-320b and si-RAD21 co–transfected HCC cells, the effects of miR-320b inhibition on these proteins were partially weakened by RAD21 silencing (Figure 6B). These data indicate that the miR-320b/RAD21 axis could affect HCC sensitivity to IR treatment in vivo.

Furthermore, the effects of the miR-320b/RAD21 axis on HCC cell tumor formation without IR treatment in the tumor xenograft model in nude mice were also determined. HCC cells pretransfected with antagomir-320b and/or si-RAD21 were subcutaneous injected into the back of nude mice, respectively. As shown in Figure S2A, the tumor volume and weight of tumors were markedly increased in the miR-320b inhibition group while decreased in RAD21-silenced HCC cells; the effects of miR-320d inhibition on tumor growth were partially reversed by RAD21 silencing. The Ki-67 and RAD21 protein expression levels were notably upregulated, and γH2AX and ATM

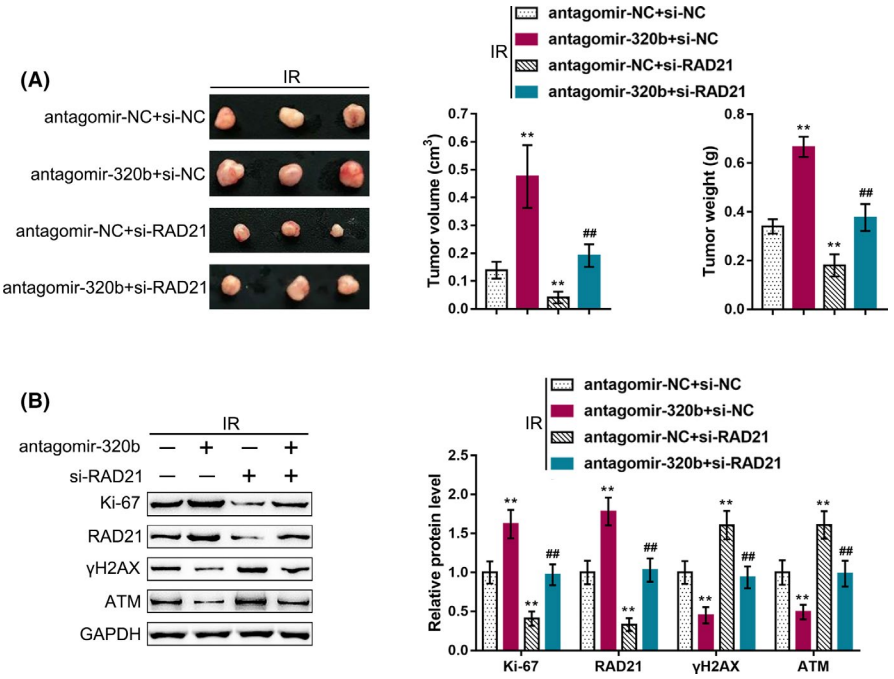

FIGURE 6 miR-320b promotes the sensitivity of hepatocellular carcinoma (HCC) to ionizing radiation (IR) treatment through RAD21. An in vivo tumor xenograft model was established in nude mice and IR treatment was performed as described. A, Tumor was harvested and photographed. Tumor volume and weight were determined. B, The protein levels of Ki-67, RAD21, γH2AX, and ATM in tumor tissues were determined by immunoblotting. One-way ANOVA followed by Tukey's test was applied for statistical analysis; $^{**}P < .01$, compared to antagomir-negative control (NC) + si-NC group; $^{\#\#}P < .01$, compared to antagomir-NC + si-RAD21 group

protein expression levels were decreased in tumors derived from miR-320b-inhibited HCC cells. In contrast, in tumors derived from RAD21-silenced HCC cells, the Ki-67 and RAD21 protein levels were dramatically restrained, and γH2AX and ATM protein levels were increased (Figure S2B). Therefore, the miR-320b/RAD21 axis affected the growth and tumorigenesis of HCC in vivo.

4 | DISCUSSION

DNA-damaging agents act as critical therapeutic interventions for cancer treatment. Nevertheless, their clinical application is sometimes limited by acquired resistance. Herein, we demonstrated that RAD21 mRNA and protein expression were increased within HCC tissue samples, particularly within IR-insensitive HCC tissues. The overexpression of RAD21 partially relieved the impact of IR on HCC by promoting the viability and suppressing the apoptosis of HCC cells. RAD21 overexpression reduced culture medium 8-OHdG concentration and decreased the protein levels of γH2AX and ATM, suggesting that RAD21 overexpression attenuated IR treatment-induced DNA damage to HCC cells. miR-320b targeted RAD21 3′-UTR to inhibit RAD21 expression. In HCC tissues, particularly in IR-insensitive HCC tissues, miR-320b expression was significantly downregulated. miR-320b inhibition also attenuated IR treatment-induced DNA damage to HCC cells; more importantly, RAD21 silencing significantly attenuated the effects of miR-320b inhibition on IR treatment-induced DNA damage, suggesting that miR-320b plays its roles through targeting RAD21.

RAD21 is an important protein for DSB repair and homologous recombination.[12,46,47] Previously, RAD21 has been regarded as one of the breast cancer anti–estrogen resistance genes, which is responsible for anti–estrogen-resistant cell proliferation.[48] Within high-grade luminal, basal, and HER2 breast carcinomas, the overexpression of RAD21 leads to impaired outcome and chemoresistance.[49] High CDKN1A and RAD21 expressions led to DNA synthesis repression and DNA damage repair, which can be regarded as two main factors leading to the resistance to cisplatin within non–small cell lung cancer.[50] Herein, the study also observed that RAD21 was abnormally expressed within HCC tissue samples compared to within adjacent normal control tissue samples. Notably, RAD21 expression was higher within IR-insensitive HCC tissue samples than within IR-sensitive tissue samples. Considering its higher expression in drug-resistant cancer cases, we speculate that RAD21 plays a potential role in HCC sensitivity to radiotherapy.

The cohesin complex is necessary for homologous recombination repair. The critical role of RAD21 in drug resistance of cancers has also been reported. Within breast carcinoma cell lines, knocking down RAD21 led to significantly reduced cell proliferation and elevated cell apoptosis. Moreover, after RAD21 silencing, the sensitivity of breast cancer MCF-7 cells to etoposide and bleomycin, two DNA-damaging chemotherapy drugs, was shown to be promoted.[19] In lung cancer cells, RAD21 overexpression could contribute to DNA damage repair caused by cisplatin.[50] Herein, RAD21 overexpression in HCC cells significantly attenuated the impact of IR-induced inhibition on cell viability and enhancement on cell apoptosis. More importantly, enhanced RAD21 also reduced the effects of IR treatment on 8-OHdG culture medium concentration, a marker of DNA oxidative damage,[51] and the protein levels of ATM and γH2AX, suggesting that RAD21 might be involved in IR-induced DNA damage.

Once the DNA repair process is disturbed, O^6-methylguanine (O6MeG) would lead to the appearance of toxic DNA-DSB because of the faulty mismatch repair when proliferating,[52] triggering apoptosis via signaling involved in ATR/ATM, the key upstream players in the DNA damage response.[53,54] Active ATM and/or ATR kinase phosphorylate several target proteins, such as histone 2AX (H2AX),[55,56] which contribute to cell cycle regulation, DSB repair, as well as autophagy and apoptosis initiation. Phosphorylation of histone variant H2AX on serine 139, forming γ-H2AX, is an early step in the cellular response to DNA damage and DNA-DSB.[57,58] Thus, ATM and γ-H2AX levels following IR treatment reflect the formation of DNA-DSB and DNA repair capacity. In the present study, RAD21 overexpression significantly attenuated IR treatment-induced increases in the protein levels of ATM and γ-H2AX, indicating that RAD21 affects HCC cell proliferation under IR treatment through acting on the formation of DNA-DSB and DNA repair processes.

There is growing evidence that miRNA will be the next crucial series of antisense therapy molecules and that they have a clear advantage over siRNA and other antisense molecules because miRNA is a naturally occurring endogenous molecule.[59] Notably, as reported, RAD21 was the target of several miRNA in numerous cancers. For example, miR-181c has been bioinformatically predicted to target RAD21 in chronic myeloid leukemia by TargetScan, miRanda, Sanger miRBase, mirTarget2, Tarbase, and PICTAR.[60] In lung cancer, RAD21 has been reported as the target of miR-92[50] and miR-21.[61] In the present study, miR-320b, which exerts a tumor-suppressive effect on lung cancer,[62] nasopharynx cancer, and[43] osteosarcoma[63], could target RAD21 to inhibit its expression. miR-320b expression itself could be induced by IR treatment. Regarding the cellular functions, miR-320b inhibition attenuated IR treatment-induced DNA damage, manifested as promoted cell viability, inhibited cell apoptosis, reduced 8-OHdG concentration, increased RAD21 protein level, and decreased ATM and γ-H2AX protein levels, indicating that inhibiting miR-320b attenuates IR sensitivity of HCC cells. When co–transfected in HCC cells under IR treatment, RAD21 silencing significantly attenuated the effects of miR-320b inhibition, indicating that miR-320b exerts its effects on HCC sensitivity to IR treatment through RAD21.

Finally, to further confirm the above-described in vitro findings, miR-320b inhibition in vivo significantly promoted while RAD21 silencing inhibited the tumor growth under IR treatment. Consistent with the in vitro results, miR-320b inhibition in vivo increased RAD21 and Ki-67 protein levels and decreased ATM and γ-H2AX protein levels in tumors, whereas RAD21 silencing in vivo exerted opposite effects on these markers. More importantly, the effects of miR-320b inhibition in vivo were also reversed by RAD21 silencing in vivo. In conclusion, we demonstrate an miR-320b/RAD21 axis modulating HCC sensitivity to IR treatment through acting on IR-induced DNA damage.

Nevertheless, the limitations of this study remain to be considered. First, there could be other miRNA sponged by RAD21 and involved in the HCC sensitivity to IR treatment. Moreover, all our experiments were carried out in mice and cells, and the research outcomes may not be directly generalized to humans. The clinical application of miR-320b or RAD21 as a potential target for HCC treatment needs to be investigated in future studies.

ACKNOWLEDGEMENTS

This study was supported by the National Natural Science Foundation of China (81602168 and 81773241), the Chinese Academy of Medical Sciences Innovation Fund (Nos. 2017-I2M-2-005 and 2017-I2M-1-005), and the National Key Research & Development Program of China (2016YFC0904600 and 2017YFC1311000).

CONFLICT OF INTEREST

All authors have read and approved the manuscript and declare that they have no competing interests.

ORCID

Jing Jin https://orcid.org/0000-0002-6645-5214

REFERENCES

1. Villanueva A. Hepatocellular Carcinoma. *N Engl J Med*. 2019;380:1450-1462.
2. Sayiner M, Golabi P, Younossi ZM. Disease burden of hepatocellular carcinoma: a global perspective. *Dig Dis Sci*. 2019;64:910-917.
3. Kulik L, El-Serag HB. Epidemiology and Management of Hepatocellular Carcinoma. *Gastroenterology*. 2019;156:477-491 e1.
4. Meyer J, Singal AG. Stereotactic ablative radiotherapy for hepatocellular carcinoma: HIstory, current status, and opportunities. *Liver Transpl*. 2018;24:420-427.
5. Yu Y, Feng M. Radiotherapy. *Semin Radiat Oncol*. 2018;28:277-287.
6. Li L, Story M, Legerski RJ. Cellular responses to ionizing radiation damage. *Int J Radiat Oncol Biol Phys*. 2001;49:1157-1162.
7. Oishi N, Wang XW. Novel therapeutic strategies for targeting liver cancer stem cells. *Int J Biol Sci*. 2011;7:517-535.
8. Wang J, Zhao H, Yu J, et al. MiR-92b targets p57kip2 to modulate the resistance of hepatocellular carcinoma (HCC) to ionizing radiation (IR)-based radiotherapy. *Biomed Pharmacother*. 2019;110:646-655.
9. McKay MJ, Troelstra C, van der Spek P, et al. Sequence conservation of the rad21 Schizosaccharomyces pombe DNA double-strand break repair gene in human and mouse. *Genomics*. 1996;36:305-315.
10. Wendt KS, Peters JM. How cohesin and CTCF cooperate in regulating gene expression. *Chromosome Res*. 2009;17:201-214.
11. Peters JM, Tedeschi A, Schmitz J. The cohesin complex and its roles in chromosome biology. *Genes Dev*. 2008;22:3089-3114.
12. Nasmyth K, Haering CH. Cohesin: its roles and mechanisms. *Annu Rev Genet*. 2009;43:525-558.
13. Grossenbacher-Grunder AM, Thuriaux P. Spontaneous and UV-induced recombination in radiation-sensitive mutants of Schizosaccharomyces pombe. *Mutat Res*. 1981;81:37-48.
14. Phipps J, Nasim A, Miller DR. Recovery, repair, and mutagenesis in Schizosaccharomyces pombe. *Adv Genet*. 1985;23:1-72.
15. Birkenbihl RP, Subramani S. Cloning and characterization of rad21 an essential gene of Schizosaccharomyces pombe involved in DNA double-strand-break repair. *Nucleic Acids Res*. 1992;20:6605-6611.
16. Birkenbihl RP, Subramani S. The rad21 gene product of Schizosaccharomyces pombe is a nuclear, cell cycle-regulated phosphoprotein. *J Biol Chem*. 1995;270:7703-7711.
17. Sonoda E, Matsusaka T, Morrison C, et al. Scc1/Rad21/Mcd1 is required for sister chromatid cohesion and kinetochore function in vertebrate cells. *Dev Cell*. 2001;1:759-770.
18. Rhodes DR, Yu J, Shanker K, et al. Large-scale meta-analysis of cancer microarray data identifies common transcriptional profiles of neoplastic transformation and progression. *Proc Natl Acad Sci U S A*. 2004;101:9309-9314.
19. Atienza JM, Roth RB, Rosette C, et al. Suppression of RAD21 gene expression decreases cell growth and enhances cytotoxicity of etoposide and bleomycin in human breast cancer cells. *Mol Cancer Ther*. 2005;4:361-368.
20. Porkka KP, Tammela TLJ, Vessella RL, et al. RAD21 and KIAA0196 at 8q24 are amplified and overexpressed in prostate cancer. *Genes Chromosomes Cancer*. 2004;39:1-10.
21. van 't Veer LJ, Dai H, van de Vijver MJ, et al. Gene expression profiling predicts clinical outcome of breast cancer. *Nature*. 2002;415:530-536.
22. Lee RC, Feinbaum RL, Ambros V. The C. elegans heterochronic gene lin-4 encodes small RNAs with antisense complementarity to lin-14. *Cell*. 1993;75:843-854.
23. Wightman B, Ha I, Ruvkun G. Posttranscriptional regulation of the heterochronic gene lin-14 by lin-4 mediates temporal pattern formation in C. elegans. *Cell*. 1993;75:855-862.
24. Bartel DP. MicroRNAs: target recognition and regulatory functions. *Cell*. 2009;136:215-233.
25. He L, Hannon GJ. MicroRNAs: small RNAs with a big role in gene regulation. *Nat Rev Genet*. 2004;5:522-531.
26. Eulalio A, Huntzinger E, Nishihara T, et al. Deadenylation is a widespread effect of miRNA regulation. *RNA*. 2009;15:21-32.
27. Wu L, Fan J, Belasco JG. MicroRNAs direct rapid deadenylation of mRNA. *Proc Natl Acad Sci U S A*. 2006;103:4034-4039.
28. Esquela-Kerscher A, Slack FJ. Oncomirs - microRNAs with a role in cancer. *Nat Rev Cancer*. 2006;6:259-269.
29. Lin S, Gregory RI. MicroRNA biogenesis pathways in cancer. *Nat Rev Cancer*. 2015;15:321-333.
30. Davis-Dusenbery BN, Hata A. MicroRNA in cancer: the involvement of aberrant microrna biogenesis regulatory pathways. *Genes Cancer*. 2010;1:1100-1114.
31. Neijenhuis S,Bajrami I, Miller R, Lord CJ, Ashworth A. Identification of miRNA modulators to PARP inhibitor response. *DNA Repair (Amst)*. 2013;12:394-402.
32. Wang Y, Huang JW, Calses P, Kemp CJ, Taniguchi T. MiR-96 downregulates REV1 and RAD51 to promote cellular sensitivity to cisplatin and PARP inhibition. *Cancer Res*. 2012;72:4037-4046.
33. Crosby ME, Kulshreshtha R, Ivan M, Glazer PM. MicroRNA regulation of DNA repair gene expression in hypoxic stress. *Cancer Res*. 2009;69:1221-1229.
34. Liang Z, Ahn J, Guo D, Votaw JR, Shim H. MicroRNA-302 replacement therapy sensitizes breast cancer cells to ionizing radiation. *Pharm Res*. 2013;30:1008-1016.
35. Kondo Y, Kimura O, Kogure T, et al. Radiation therapy is a reasonable option for improving the prognosis in hepatocellular carcinoma. *Tohoku J Exp Med*. 2015;237:249-257.
36. Ma J, Zeng S, Zhang Y, et al. BMP4 promotes oxaliplatin resistance by an induction of epithelial-mesenchymal transition via MEK1/ERK/ELK1 signaling in hepatocellular carcinoma. *Cancer Lett*. 2017;411:117-129.
37. Llovet JM, Di Bisceglie AM, Bruix J, et al. Design and endpoints of clinical trials in hepatocellular carcinoma. *J Natl Cancer Inst*. 2008;100:698-711.
38. Zhang Y, Zheng L, Huang J, et al. MiR-124 Radiosensitizes human colorectal cancer cells by targeting PRRX1. *PLoS One*. 2014;9:e93917.

39. Kunej T, Godnic I, Horvat S, Zorc M, Calin GA. Cross talk between microRNA and coding cancer genes. *Cancer J*. 2012;18:223-231.
40. Chen JQ, Ou YL, Huang ZP, Hong YG. MicroRNA-212-3p inhibits the proliferation and invasion of human hepatocellular carcinoma cells by suppressing CTGF expression. *Sci Rep*. 2019;9:9820.
41. Ying J, Yu X, Ma C, Zhang Y, Dong J. MicroRNA-363-3p is downregulated in hepatocellular carcinoma and inhibits tumorigenesis by directly targeting specificity protein 1. *Mol Med Rep*. 2017;16:1603-1611.
42. Jiang X, Shen X. Knockdown of miR-299-5p inhibits the progression of hepatocellular carcinoma by targeting SIAH1. *Bull Cancer*. 2018;105:873-883.
43. Li Y, Tang X, He Q, et al. Overexpression of mitochondria mediator gene TRIAP1 by miR-320b loss is associated with progression in nasopharyngeal carcinoma. *PLoS Genet*. 2016;12:e1006183.
44. Xu J, Lin H, Li G, et al. The miR-367-3p increases sorafenib chemotherapy efficacy to suppress hepatocellular carcinoma metastasis through altering the androgen receptor signals. *EBioMedicine*. 2016;12:55-67.
45. Sun S, Wang X, Xu X, et al. MiR-433-3p suppresses cell growth and enhances chemosensitivity by targeting CREB in human glioma. *Oncotarget*. 2017;8:5057-5068.
46. Feeney KM, Wasson CW, Parish JL. Cohesin: a regulator of genome integrity and gene expression. *Biochem J*. 2010;428:147-161.
47. Potts PR, Porteus MH, Yu H. Human SMC5/6 complex promotes sister chromatid homologous recombination by recruiting the SMC1/3 cohesin complex to double-strand breaks. *EMBO J*. 2006;25:3377-3388.
48. van Agthoven T, Sieuwerts AM, Meijer D, et al. Selective recruitment of breast cancer anti–estrogen resistance genes and relevance for breast cancer progression and tamoxifen therapy response. *Endocr Relat Cancer*. 2010;17:215-230.
49. Xu H, Yan M, Patra J, et al. Enhanced RAD21 cohesin expression confers poor prognosis and resistance to chemotherapy in high grade luminal, basal and HER2 breast cancers. *Breast Cancer Res*. 2011;13:R9.
50. Zhao J, Fu W, Liao H, et al. The regulatory and predictive functions of miR-17 and miR-92 families on cisplatin resistance of non–small cell lung cancer. *BMC Cancer*. 2015;15:731.
51. Kasai H. Analysis of a form of oxidative DNA damage, 8-hydroxy-2'-deoxyguanosine, as a marker of cellular oxidative stress during carcinogenesis. *Mutat Res*. 1997;387:147-163.
52. Roos W, Baumgartner M, Kaina B. Apoptosis triggered by DNA damage O6-methylguanine in human lymphocytes requires DNA replication and is mediated by p53 and Fas/CD95/Apo-1. *Oncogene*. 2004;23:359-367.
53. Kaina B, Christmann M, Naumann S, et al. MGMT: key node in the battle against genotoxicity, carcinogenicity and apoptosis induced by alkylating agents. *DNA Repair (Amst)*. 2007;6:1079-1099.
54. Eich M, Roos WP, Nikolova T, et al. Contribution of ATM and ATR to the resistance of glioblastoma and malignant melanoma cells to the methylating anticancer drug temozolomide. *Mol Cancer Ther*. 2013;12:2529-2540.
55. Burma S, Chen BP, Murphy M, et al. ATM phosphorylates histone H2AX in response to DNA double-strand breaks. *J Biol Chem*. 2001;276:42462-42467.
56. Nojima H. Protein kinases that regulate chromosome stability and their downstream targets. *Genome Dyn*. 2006;1:131-148.
57. Rogakou EP, Pilch DR, Orr AH, et al. DNA double-stranded breaks induce histone H2AX phosphorylation on serine 139. *J Biol Chem*. 1998;273:5858-5868.
58. Harper JW, Elledge SJ. The DNA damage response: ten years after. *Mol Cell*. 2007;28:739-745.
59. Fromm B, Billipp T, Peck LE, et al. A uniform system for the annotation of vertebrate microRNA genes and the evolution of the human microRNAome. *Annu Rev Genet*. 2015;49:213-242.
60. Mosakhani N, Mustjoki S, Knuutila S. Down-regulation of miR-181c in imatinib-resistant chronic myeloid leukemia. *Mol Cytogenet*. 2013;6:27.
61. Wang Q, Zhang L. Possible molecular mechanisms for the roles of microRNA-21 played in lung cancer. *Technol Cancer Res Treat*. 2019;18:1533033819875130.
62. Zhang S, Zhang X, Sun Q, et al. LncRNA NR2F2-AS1 promotes tumourigenesis through modulating BMI1 expression by targeting miR-320b in non–small cell lung cancer. *J Cell Mol Med*. 2019;23:2001-2011.
63. Lv GY, Miao J, Zhang XL. Long noncoding RNA XIST promotes osteosarcoma progression by targeting Ras-related protein RAP2B via miR-320b. *Oncol Res*. 2018;26:837-846.

SUPPORTING INFORMATION

Additional supporting information may be found online in the Supporting Information section.

How to cite this article: Wang J, Zhao H, Yu J, et al. MiR-320b/RAD21 axis affects hepatocellular carcinoma radiosensitivity to ionizing radiation treatment through DNA damage repair signaling. *Cancer Sci*. 2021;112:575–588. https://doi.org/10.1111/cas.14751